OXFORD

International Journal of Neuropsychopharmacology, 2025, pyaf042

https://doi.org/10.1093/ijnp/pyaf042

Advance access publication 19 June 2025

Regular Research Article

Regular Research Article

Predicting antidepressant responsiveness in major depressive disorder patients via electroencephalography gamma-band dynamic functional connectivity in response to salient auditory stimuli

Kang-Min Choi, PhD[1,2], Taegyeong Lee, BS[1], Seung-Hwan Lee, MD, PhD[2,3,4,*], Chang-Hwan Im, PhD[1,5,*]

[1]Department of Electronic Engineering, Hanyang University, Seoul 04763, Republic of Korea
[2]Clinical Emotion and Cognition Research Laboratory, Inje University, Goyang, Gyeonggi-do 10380, Republic of Korea
[3]Department of Psychiatry, Ilsan Paik Hospital, Inje University College of Medicine, Goyang, Gyeonggi-do 10380, Republic of Korea
[4]Bwave Inc, Goyang, Gyeonggi-do 10380, Republic of Korea
[5]Department of Biomedical Engineering, Hanyang University, Seoul 04763, Republic of Korea
*Corresponding authors: Chang-Hwan Im, PhD, Departments of Electronic Engineering and Biomedical Engineering, Hanyang University, 222 Wangsimni-ro, Seongdong-gu, Seoul 04763, Republic of Korea (ich@hanyang.ac.kr) and Seung-Hwan Lee, MD, PhD, Department of Psychiatry, Inje University Ilsan Paik Hospital, Inje University, 180, Juhwa-ro, Ilsanseo-gu, Goyang-si, Gyeonggi-do, Republic of Korea (lshpss@paik.ac.kr)

Abstract

Background: Heterogeneous pathophysiological characteristics in patients with major depressive disorder (MDD) lead to individually differentiated sensitivities to antidepressants. Based on the hypothesis that gamma-band dynamic fluctuations in cortical functional connectivity (FC) in response to salient stimuli are linked to pathophysiological characteristics, we conducted a classification analysis for antidepressant responsiveness prediction.

Methods: Biosignals and psychological measures were acquired from 47 patients with MDD prior to treatment. After 8 weeks of antidepressant therapy, patients were divided into non-remitted MDD (nrMDD; aged 42.55 ± 11.52 years; $n = 20$) and remitted MDD (rMDD; aged 47.22 ± 11.59 years; $n = 27$) groups based on their depressive symptom reduction. Electroencephalography (EEG) signals were acquired during the duration-variant auditory mismatch negativity paradigm. From the deviant condition, gamma-band weighted phase-lag index-based dynamic fluctuations were evaluated using a template generated from 21 demography-matched healthy control (aged 43.81 ± 14.10 years) data.

Results: Using these dynamic functional connectivity (dFC) features, a machine learning-based classification analysis was performed for nrMDD and rMDD. Using leave-one-out cross-validation, the linear discriminant analysis classifier achieved the best accuracy (82.98%) for classifying nrMDD and rMDD. Further simple effect analyses identified three core dFC features for nrMDD: (i) relatively intact time-dependent FC between the left frontal and right temporal regions; (ii) disrupted right frontoparietal FC; and (iii) disrupted left fronto-temporal FC. These dFC features commonly exhibit transient hyperconnections in patients with nrMDD.

Conclusions: We demonstrated that gamma-band dFC responses to salient stimuli could serve as potential biomarkers for antidepressant responsiveness prediction in patients with MDD.

Keywords: electroencephalography; major depressive disorder; antidepressant responsiveness; dynamic functional connectivity; mismatch negativity.

Significance Statement

Predicting antidepressant responsiveness in patients with major depressive disorder (MDD) remains a clinical challenge due to their heterogeneous pathophysiology. Here, we propose that aberrant gamma-band dynamic functional connectivity (dFC) during auditory mismatch negativity experimental paradigm may serve as potential biomarkers for predicting antidepressant responsiveness. Using machine learning classifiers, we demonstrated that these dFC measures acquired during the baseline period could classify patients as non-remitted MDD or remitted MDD. Further statistical analyses suggest that transient inter-regional hyperactivity contributed to this result, potentially associated with *N*-methyl-D-aspartate receptor dysfunction. Consistent with previous static FC findings, non-remitted MDD could be characterized by altered functional network patterns compared to demographically matched healthy controls. These results suggest that pre-treatment gamma-band dFC features could provide objective neural markers, facilitating future treatment planning in MDD.

Received for publication: March 8, 2025. **Accepted:** June 18, 2025. **Editorial decision:** June 17, 2025.

INTRODUCTION

Prediction of antidepressant responsiveness in patients with major depressive disorder (MDD) remains a critical challenge. Although antidepressant treatment is one of the foremost therapies, ~20%-30% of patients do not respond favorably to it.[1,2] This empirical, trial-and-error treatment approach can expose treatment-resistant patients to unnecessary side effects of medicines that significantly influence the central nervous system.[3] Numerous clinical studies have indicated that antidepressant responsiveness is associated with various heterogeneities in patients with MDD. For instance, those who exhibit more severe clinical symptoms involving functional brain networks, such as anhedonia, attentional deficits, or socio-affective impairments, tend to show greater resistance to pharmacotherapy.[4-6] This led to the hypothesis that MDD encompasses several subtypes with diverse pharmacotherapeutic responsiveness.

Neuroimaging studies are advantageous for subtype analyses. They offer pathophysiological insights into treatment-resistance traits by providing objective neurobiological evidence. Among various neuroimaging modalities, electroencephalography (EEG) is a promising tool for investigating biomarkers to predict antidepressant responsiveness prior to treatment. Specifically, EEG directly captures complex neurophysiological activities with superior temporal resolution compared to functional magnetic resonance imaging (fMRI).[7,8] Several EEG-based studies have demonstrated that treatment responsiveness can be predicted via various neural patterns, such as power spectral density (PSD), event-related potential, and functional connectivity (FC).[9-13] Despite this potential, prediction of antidepressant responsiveness remains challenging. Although most pathophysiological findings have been validated statistically, there is a need for validation at the individual level to develop practical clinical applications.

Previous EEG-based studies have demonstrated that machine learning (ML)-based classifiers could predict antidepressant responsiveness.[9,10,14-18] These studies generally integrated feature candidates derived from both the baseline (ie, 0th week) and early treatment phases (1st or 2nd week) to enhance the classification performance.[9,15-17] However, these short periodic antidepressant dosages can also significantly influence the central nervous system,[19,20] potentially causing side effects owing to neurotransmitter activity modulation. Moreover, the reported performance by some studies was inflated owing to wrong validation processes, such as information leakage or overfitting.

Expanding the number of biomarker candidates could be a breakthrough in the development of reliable predictive systems. Although most previous ML-based studies primarily utilized resting-state PSD-related features, recent suggestions indicate that a combination of diverse biomarkers could enhance the ML performance by capturing the heterogeneous characteristics of individual patients with MDD.[10,17,21] In particular, it is well known that various well-established EEG biomarkers derived from passive experimental paradigms, which do not require overt behavioral responses, reflect distinct pathophysiological characteristics of MDD. For example, duration-variant auditory mismatch negativity (MMN) is influenced by disrupted *N*-methyl-D-aspartate receptor (NMDAR) activity in MDD.[22,23] Furthermore, it is worth noting that the MMN paradigm offers emotionally neutral yet salient stimuli, enabling the exploration of neural mechanisms involved in salient information processing and the expansion of clinically relevant biomarker candidates. For instance, gamma-band EEG activity, which is known to involve temporal synchronization across cortical networks influenced by NMDAR functioning,[24-27] potentially provides neurophysiological information regarding dynamic cortical communication during these cognitive processes.

Non-zero phase-lag gamma-band inter-regional synchronizations have recently been suggested to play a role in feed-forward communication.[28,29] This high-frequency band is particularly advantageous for assessing neural dynamics. Technically, it can provide sufficient oscillations for reliable frequency analysis within the limited temporal windows. Furthermore, neurobiologically, it is not only associated with the NMDAR functioning, but also suitable for reflecting dynamic neural processes.[30,31] Nevertheless, various studies have analyzed gamma-band networks on the assumption of stable connectivity patterns,[1,12,32] reporting that treatment-resistant MDD generally exhibits more altered neural pathways. Unlike this static network assumption, dynamic functional connectivity (dFC) captures time-varying changes in inter-regional interactions, offering insights into transient neural communication patterns. Therefore, investigating dFC patterns may broaden the understanding of pathophysiology underlying antidepressant treatment resistance, serving as novel biomarkers.

In this study, we investigated whether pre-treatment FC dynamics in response to salient stimuli can predict antidepressant responsiveness. Specifically, gamma-band dFC was evaluated to capture transient information flow and then employed as a feature candidate to discriminate between non-remitted MDD (nrMDD) and remitted MDD (rMDD) under the MMN paradigm. The feasibility of dFC features was demonstrated using ML-based classification models. Further statistical analyses and pathophysiological interpretations were conducted to identify powerful features. We hypothesized that patients with nrMDD would exhibit aberrant salient information processing, which is associated with their pathophysiological characteristics.

METHODS

Participants

A total of 51 patients with drug-naïve MDD (aged 45.22 ± 12.20 years; Males: 3) were enrolled in the study from the Department of Psychiatry at the Inje University, Ilsan Paik Hospital. Diagnoses were made by board-certified psychiatrists based on the Structured Clinical Interview for the DSM-5. None of the patients had any history of neurological illness, intellectual disability, substance abuse, traumatic brain injury, psychotic disorder, bipolar disorder, personality disorder, post-traumatic stress disorder, obsessive compulsive disorder, or hearing impairment. Furthermore, none of the patients were pregnant. They refrained from taking any psychotropic medication for at least 1 month prior to data acquisition.

After data acquisition, antidepressant treatment, either vortioxetine or escitalopram, was administered for 8 weeks. Participants received 10 mg po for the 1st week, which was then flexibly adjusted to a range of 10-20 mg po until the 8th week. Afterward, the patients were divided into two groups according to their depressive symptom severity level at the end of treatment, based on the Hamilton Depression Rating Scale for the 8th week (Ham-D_8; details in the following section): (i) nrMDD (Ham-$D_8 \geq 8$, $n = 20$) and (ii) rMDD (Ham-$D_8 < 8$, $n = 27$). It should be noted that data analysis was conducted with 47 patients with MDD (aged 46.61 ± 10.05 years; Males: 3) due to data quality issues (details in the Supplementary Material). Several patients had comorbidities: panic disorder (nrMDD = 4 vs. rMDD = 8), insomnia (3 vs. 6),

adjustment disorder (1 vs. 4), agoraphobia (2 vs. 1), anxiety disorder (0 vs. 2), neurotic disorder (1 vs. 0), dysthymia (1 vs. 0), somatization (0 vs. 1), and palpitation (0 vs. 1).

In addition, a total of 22 healthy controls (HCs; aged 46.61 ± 14.00 years; Males: 3) were recruited from the local community using flyers and posters. None had any major psychiatric or neurological disorders, head injuries, or hearing impairment. Furthermore, they had no family history of psychiatric disorders. Due to data quality issues, one participant was excluded from further analysis. As a result, the data from 21 HCs (aged 43.81 ± 14.10 years; Males: 3) were analyzed.

This study was conducted in accordance with the Declaration of Helsinki. All individuals provided written informed consent and fully understood the nature of the experiment prior to their participation. Ethical review and approval of this study were obtained from the Inje University, Ilsan Paik Hospital Institutional Review Board (Nos. 2016-08-017-007 and 2015-04-316-019).

Psychiatric Measures

To assess depressive and anxiety symptom severity, the Hamilton Depression Rating Scale (Ham-D) with 17 items[33] and the Hamilton Anxiety Rating Scale (Ham-A) with 14 items[34] were employed. In addition, to assess psychomotor and working memory processing speed, the Digit-Symbol Substitution Test (DSST)[35] was employed. These psychiatric measures were obtained at the baseline (ie, 0th week) and after the treatment (ie, 8th week).

Experimental Paradigm

All participants engaged in a duration-variant auditory MMN paradigm. The probability of a deviant stimulus was set to 10% for 750 trials. The participants were asked to watch a silent movie (Charlie Chaplin silent film) during auditory stimulus presentation without focusing on the auditory stimuli. Auditory stimuli were presented binaurally using noise-canceling MDR-D777 headphones (Sony, Tokyo, Japan). The pitch and loudness of all stimuli were set to 1000 Hz and 85 dB, respectively. The interstimulus interval was fixed at 600 ms. The duration of the stimulation was set to 50 ms for the standard stimuli and 100 ms for the deviant stimuli, with the rising and falling edges set to 10 ms. The detailed information is accessible in our previous study.[13]

Signal Acquisition

The participants were asked to sit comfortably on a chair. Biosignals were acquired using Neuroscan SynAmps2 (Compumedics, El Paso, TX, USA). A total of 64 Ag-AgCl electrodes mounted on a QuikCap were placed according to the extended 10-20 system to record the EEG signals. To record the horizontal and vertical electrooculogram components, four additional electrodes were placed on the outer canthi above and below the left eye. An additional channel was attached below the clavicle to record the electrocardiogram signals. The impedance of all electrodes was maintained below 5 kΩ during the recording. Biosignals were recorded at a 1000-Hz sampling rate, before applying a bandpass filter with cutoff frequencies of 0.1 and 100 Hz. A 60-Hz notch filter was applied to reject power-line noise.

Signal Pre-Processing

The acquired EEG signals were pre-processed using the EEGLAB toolbox[36] in MATLAB R2023a (MathWorks, Natick, MA, USA). The EEG signals were pre-processed using independent component analysis, bandpass filtering between 0.1 and 50 Hz, bad block removal, and bad channel interpolation (further details can be found in the Supplementary Material). The cleaned EEG signals were segmented into 700 ms, ranging from −100 to 600 ms according to the stimulus onset. Subsequently, the signals were detrended and baseline-corrected. Among them, 45 deviant condition segments were randomly selected from those with absolute maximum amplitudes of less than 75 μV.

Construction of the Dynamic Functional Network

To construct functional brain networks, source-level signals were reconstructed using the Brainstorm toolbox.[37] From the common-average referenced sensor-level EEG signals, source activities were calculated using a depth-weighted L2-norm estimator. The lead field matrix was acquired for 15 002 cortical voxels based on the Colin27 MRI brain template using a three-layer boundary element model implemented in the OpenMEEG project software.[38]

A total of 31 cortical regions were used as representative functional nodes. These regions of interest (ROIs) were determined based on previous resting-state fMRI studies.[1,39,40] Their representative source activities were reconstructed as the first principal components of the neighboring voxels within a 5-mm Euclidean distance from their representative Montreal Neurological Institute coordinates. Whole-brain ROIs were included in one of the six modules (Table S1 and Figure S1): (i) visual network (VN; R1–R2); (ii) somatosensory network (R3–R4); (iii) dorsal attention network (R5–R12); (iv) default mode network (DMN; R13–R16); (v) central executive network (CEN; R17–R24); and (vi) salience network (R25–R31).

Hilbert-transform-based weighted phase-lag indices (wPLIs; Supplementary Material)[41,42] were evaluated between pairs of nodes for the gamma band as FCs (ie, edges). The reconstructed source-level segments were bandpass-filtered between 30 and 50 Hz using a sixth-order Butterworth filter. To assess the dynamic fluctuations of the FCs, wPLIs were calculated for every 5-ms time point using a 150-ms rectangular sliding window with 10 ms at both ends being eliminated to minimize edge effects. The wPLIs were calculated between 0 and 500 ms within each segment to minimize stimulus-irrelevant effects. It should be noted that among the various frequency bands, gamma-band analysis is the only methodologically reliable within the short temporal window used in this study, as fewer than four oscillations are captured for frequency components lower than 30 Hz. To mitigate noise and artifactual effects, we averaged the time-variant wPLIs across the randomly selected 45 epochs.

To evaluate the temporal dynamics of FCs, a template was created using demography-matched HC data. Specifically, the "normative" template was acquired by grand-averaged time-dependent wPLIs of HCs. Pearson correlations were computed across time points (0-500 ms) between the template and each patient's time-dependent wPLI trajectories for every pair of nodes. This approach was carefully designed to efficiently compress the feature space while capturing this pathophysiological characteristic, without relying on prior information about the dataset.

Pearson correlation coefficients were computed between the template and the corresponding time-dependent wPLIs for each patient for dFC evaluation. The correlation coefficients were then Fisher's r-to-z transformed for the distribution to follow normality (Supplementary Material). Ultimately, 465 dFC feature candidates (ie, all possible edges among 31 nodes) were extracted from each patient.

ML-Based Classification Analysis

An ML-based classification analysis was performed to demonstrate the potential of dFC features. Three types of classification models, namely, linear discriminant analysis (LDA), k-nearest

neighbors (KNNs), and support vector machine, were employed for nrMDD and rMDD classification. The model hyperparameters were set as their default values (Supplementary Material), except for the number of neighbors for the KNN model, which ranged from 2 to 10. Leave-one-out cross-validation (LOOCV) was used to validate the classifier performance. For each fold ($n = 47$), a maximum of five features were independently selected from the training set to prevent dimensionality-related overfitting. Specifically, from the 465 dFC feature candidates, we selected those with the top Fisher scores, calculated as the ratio of between-class variance to within-class variance.[43] It should be noted that no other feature candidates, aside from dFCs, were included in constructing the ML models.

To prevent bias due to sample imbalance, the misclassification cost was set as the inverse ratio of patients in each group (ie, 0.5745 and 0.4255 for nrMDD and rMDD, respectively). To assess the classification performance, classification accuracy, sensitivity, and specificity were calculated with respect to nrMDD. Finally, the receiver operating characteristic (ROC) curve was acquired for the outperforming classifier.

Statistical Analysis

It was assumed that all data followed a normal distribution because all absolute values of skewness and kurtosis were less than two and seven, respectively.[44] Demographic data were compared among the three groups, including nrMDD, rMDD, and HC, using a *t*-test for age and education and a Chi-squared test for gender. Psychiatric measures were compared between the nrMDD and rMDD groups using *t*-tests.

A simple effect analysis was employed for "core" dFC features, which were most frequently selected in the LOOCV step. The core dFCs between the nrMDD and rMDD groups were compared using a permutation test ($n = 5000$) to avoid multiple correction issues.[45] A further cluster-based permutation test ($n = 5000$) was employed along the temporal dimension to identify specific time ranges contributing to significant group differences.[46] Furthermore, a Pearson correlation analysis was performed between the core dFCs and the change ratio of Ham-D between pre- and post-treatment (Supplementary Material). A bias-corrected and accelerated bootstrap resampling technique ($n = 5000$) was used to avoid multiple comparison issues and to account for potential bias and skewness.[47] The statistical tests were performed using SPSS 27 (SPSS, Inc., Chicago, IL, USA) and MATLAB R2023a (MathWorks, Natick, MA, USA).

RESULTS

Demographic and Psychological Measures

There were no significant demographic differences between the groups (*P*s > .05; Table 1). Furthermore, there were no significant differences in baseline psychiatric measures between the nrMDD and rMDD groups (*P*s > .05).

Classification Analysis

In the classification analysis, the best classification performance was achieved when the LDA classifier was employed with three features. Specifically, we achieved classification accuracy, sensitivity, and specificity of 82.98%, 95.00%, and 74.07%, respectively. The area under the curve (AUC) for the ROC curve was 0.8315 (Figure 1A). Among the dFC feature candidates, three of them were most frequently selected (Figure 1B): (i) between the left posterior middle frontal gyrus and right supramarginal gyrus (referred to as lPMFG–rSup; $n = 47$); (ii) between the right angular gyrus and right anterior middle frontal gyrus (rAng–rAMFG; $n = 47$); and (iii) between the left primary visual cortex and left middle temporal gyrus (lV1–lMTG; $n = 45$). Therefore, these three dFCs were regarded as core features for further analysis.

Statistical Analysis

Group comparisons were performed exclusively for the three core dFC features. In the simple effect analyses, permutation test results revealed that nrMDD showed increased dFC in the lPMFG–rSup (nrMDD = 0.2742 > rMDD = 0.0181; *P*=.001, Figure 2A) but decreased dFCs in the rAng–rAMFG (nrMDD = −0.0271 < rMDD = 0.2336; *P*=.015, Figure 2B) and lV1–lMTG (nrMDD = −0.0424 < rMDD = 0.1835; *P*=.007, Figure 2C) compared to rMDD (Figure 1B). Further cluster-based permutation test results identified significantly increased time-dependent wPLIs between the lPMFG and rSup, ranging from 195 to 265 ms (*P*=.0203, Figure 2A), and between the rAng and rAMFG, ranging from 0 to 40 ms (*P*=.0437, Figure 2B), in patients with nrMDD. No other significant intergroup differences were observed.

In the correlation analyses, there was a positive correlation between dFC in the lPMFG–rSup and the Ham-D change ratio ($r = 0.485$; *P*=.001; 95% confidence interval (CI): 0.313-0.624; Figure 3A). In addition, there was a negative dFC correlation between the lV1–lMTG and Ham-D ratio ($r = -0.291$; *P*=.047; 95% CI: −0.537 to −0.069; Figure 3B).

DISCUSSION

In this study, we investigated the potential of dFC in response to salient stimuli as an antidepressant responsiveness predictor in patients with MDD. It was demonstrated that the dFC features could effectively discriminate between nrMDD and rMDD. Specifically, HC template-based analyses indicated that patients with nrMDD were characterized by intact time-dependent FC patterns in the lPMFG–rSup but disrupted patterns in the rAng–rAMFG and lV1–lMTG. Among them, increased lV1–lMTG dFC and decreased lPMFG–rSup similarities were associated with the improvement in depressive symptoms.

Methodologically, HC template-based Pearson correlation analyses were used to evaluate FC dynamics for each patient. Pearson's correlation was employed to effectively capture the time-dependent characteristics. It is to be noted that Pearson's correlation was employed to evaluate FC in fMRI studies based on this trait.[48] In addition, the correlation-based analytical approach was developed following recent resting-state functional network findings reporting that patients showing intact, namely similar to HC, FC patterns generally respond better to antidepressant.[2,11,49] Indeed, patients with nrMDD exhibit remarkably altered FC dynamics (Figure S2). Our findings not only support but also expand upon the findings of previous studies: patients with MDD exhibiting intact FC dynamics as well as resting-state connectomes might respond more sensitively to pharmacotherapy. In particular, two of the three core features (rAng–rAMFG and lV1–lMTG) corroborated this hypothesis.

Aberrant gamma-band dFCs have been hypothesized to be linked to the NMDAR model. Recent molecular psychiatric studies have focused on excessive NMDAR activation in patients with MDD.[50,51] For example, ketamine, an NMDAR antagonist, has been reported to rapidly improve depressive symptom severity.[51,52] Furthermore, it is widely accepted that NMDAR malfunctioning contributes to aberrant gamma-band activity.[26,27] Given that gamma-band activity plays a crucial role in precise temporal

Table 1. Demographic and symptom severity comparison. While the demographic measures, including age, gender, and education were compared for three groups, the clinical measures were compared between nrMDD and rMDD groups.

	nrMDD ($n = 20$)	rMDD ($n = 27$)	HC ($n = 21$)	P
Age	42.55 ± 11.52	47.22 ± 11.99	43.81 ± 14.10	.416
Gender (M/F)	1/19	2/25	3/18	.546
Education	13.35 ± 2.88	13.44 ± 3.07	13.43 ± 4.19	.995
Ham-D				
Week 0	29.11 ± 5.78	25.44 ± 6.57		.054
Week 8	16.90 ± 9.11	3.67 ± 2.02		<.001
Ham-A				
Week 0	26.60 ± 6.15	24.59 ± 5.46		.244
Week 8	17.15 ± 8.28	3.59 ± 2.71		<.001
DSST				
Week 0	32.70 ± 15.10	32.93 ± 15.51		.960
Week 8	37.44 ± 16.71	34.35 ± 14.10		.510

Abbreviations: nrMDD, non-remitted MDD; rMDD, remitted MDD; HC, healthy control; Ham-D, Hamilton Depression Rating Scale; Ham-A, Hamilton Anxiety Rating Scale; DSST, Digit-Symbol Substitution Test.

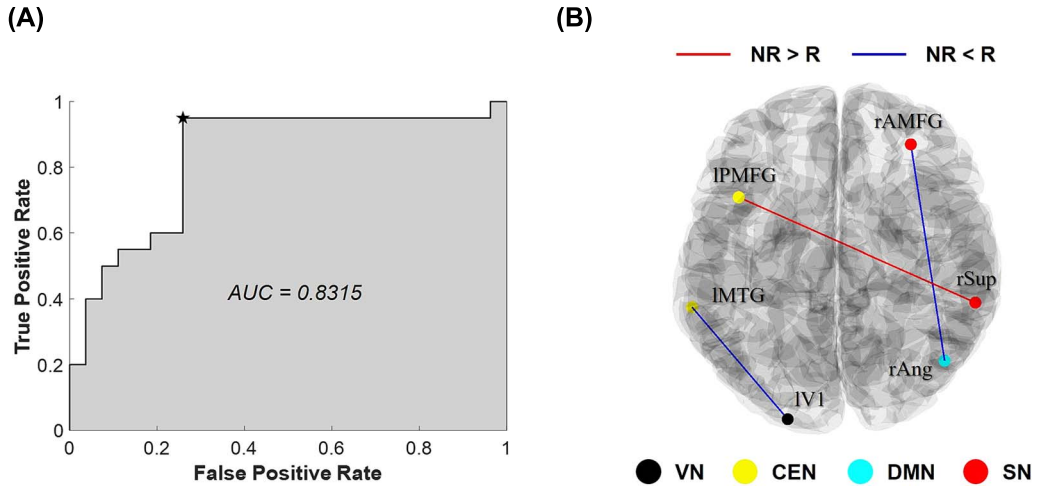

Figure 1. Best classification performance and core feature subset. (A) ROC curve with its classifier AUC. The star indicates the selected criterion of the model. (B) Core features. Nodes belong to four functional networks: VN – lV1; CEN – lPMFG; DMN – rAng, lMTG; SN – rAMFG, rSup (refer to Figure S1). dFC between lPMFG and rSup was increased in the nrMDD group compared to the rMDD group, whereas all other connections showed reduced dFC in nrMDD. ROC: Receiver operating characteristic; AUC: area under the curve; l-: left hemispheric; r-: right hemispheric; AMFG: anterior middle frontal gyrus; PMFG: posterior middle frontal gyrus; Sup: supramarginal gyrus; MTG: middle temporal gyrus; V1: primary visual cortex; Ang: angular gyrus; NR: non-remitted MDD; R: remitted MDD.

synchronization across cortical networks,[24,25] we propose that gamma-band FC dynamics could provide a sensitive NMDAR malfunctioning measure. Abnormal hyperconnections were observed for lPMFG–rSup and rAng–rAMFG (Figure 2A and B, respectively), which supports our hypothesis.

dFC features, including rAng–rAMFG and lV1–lMTG, were disrupted in patients with nrMDD. The aberrant dynamics between rAng and rAMFG may stem from hyperconnectivity during the initial period (0-40 ms, Figure 2B). rAMFG, an anterior part of the dorsolateral prefrontal cortex (DLPFC) in the right hemisphere,[53] is one of the main targets of transcranial electric or magnetic neuromodulation therapy.[54] It is widely accepted that right DLPFC hyperactivation increases withdrawal motivation.[55] Furthermore, efficient information transmission may be hindered by the initial hyperconnection period with rAng, a central region of the DMN, which should be deactivated according to external stimuli.[56] In contrast, the dFC of the left hemispheric temporo-occipital region (ie, lMTG and lV1) might reflect the flexibility of the functional network. The interaction between the VN and CEN modules is not thought to be directly involved in salient processing; instead, this dFC feature might display appropriate inhibitory functioning. Specifically, nrMDD exhibited increased wPLIs within 200-300 ms, whereas others exhibited decreased wPLIs. This range coincided with the temporal window in which the MMN component is typically observed, suggesting a potential impairment in efficient reconfiguration for salient processing.

Contrary to the findings of other studies, the lPMFG–rSup dFC was altered in patients with rMDD but not in those with nrMDD. Although patients with intact FC patterns generally show antidepressant responsiveness, as mentioned previously, there are a few contradictory FCs.[49] Several factors may have contributed to this result. The first is the NMDAR model. The higher temporal correlation for nrMDD might have resulted from hyperconnectivity ranging from 195 to 265 ms (Figure 2A). Despite the opposite trend of the other core dFC features, this result is ultimately consistent with the other dFCs. The second is the ceiling effect. Interestingly, the lPMFG–rSup dFC exhibited a significant mediating effect between the Ham-D change ratio ($r = 0.485$; $P = .001$; 95% CI: 0.313-0.624; Figure 3) and pre-treatment DSST score ($r = 0.270$; $P = .067$; 95% CI: 0.025-0.498; Figure 4). Although no direct significant correlation was observed between the Ham-D change ratio and pre-treatment DSST score ($P > .1$), the lPMFG–rSup dFC mediated a

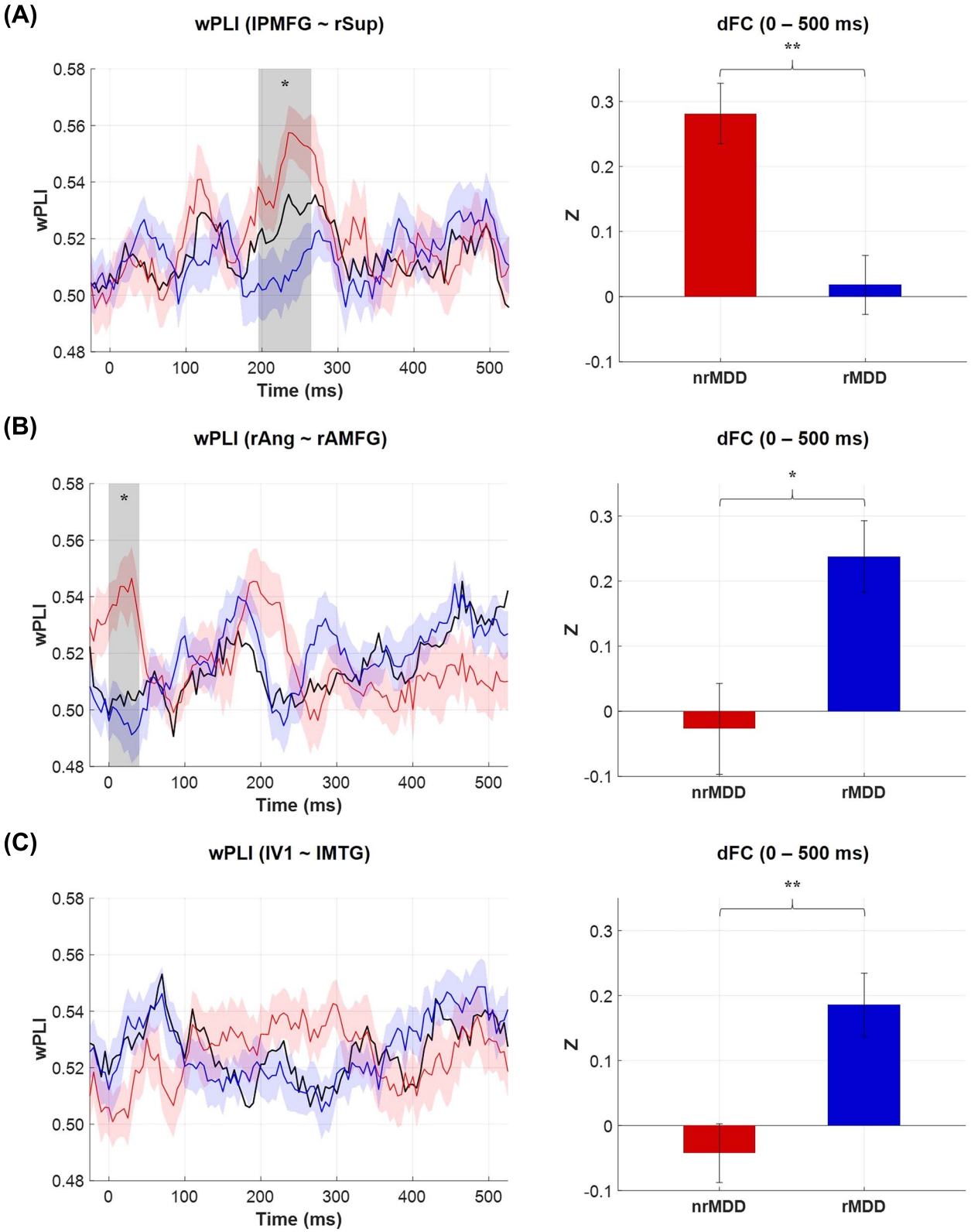

Figure 2. Comparison between core dFC features. The left panels illustrate the temporal dynamics of the FCs for nrMDD, rMDD, and HC. Their time-dependent wPLIs are displayed with standard errors for both MDD groups shaded. The time intervals in which nrMDD and rMDD showed significant differences are highlighted with shaded areas based on the cluster-based permutation test. The right panels display the group comparisons for the dFCs. (A) dFC comparison in the lPMFG–rSup. (B) dFC comparison in the rAng–rAMFG. (C) dFC comparison in the lV1–lMTG. It should be noted that ML classification and statistical analyses were conducted using overall dFC measures shown in the right panels. *P < .05; **P < .01. L-: left; r-: right; AMFG: anterior middle frontal gyrus; PMFG: posterior middle frontal gyrus; Sup: supramarginal gyrus; MTG: middle temporal gyrus; V1: primary visual cortex; Ang: angular gyrus; nrMDD: non-remitted MDD; rMDD: remitted MDD; wPLI: weighted phase-lag index.

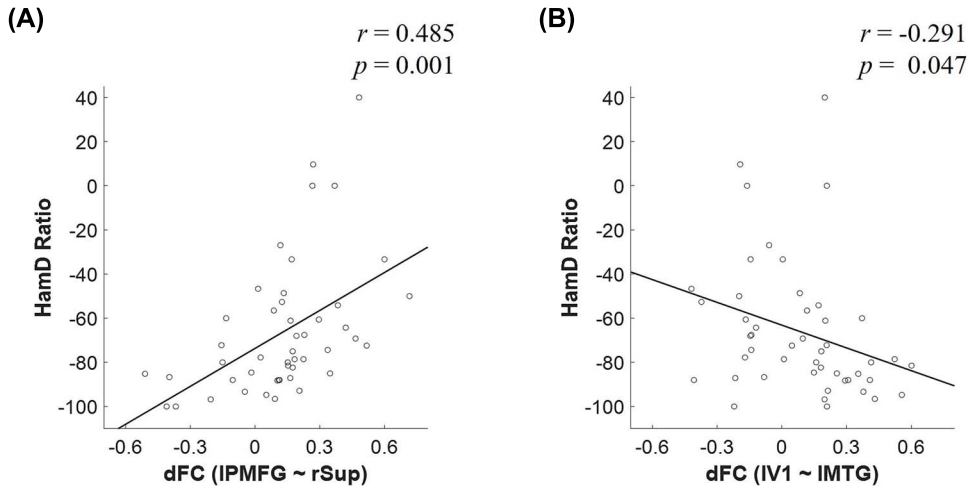

Figure 3. Correlations between the core dFCs and the Ham-D change ratio. (A) Correlation result of the dFC in the lPMFG–rSup. (B) Correlation result of the dFC in the lV1–lMTG. It should be noted that a negative Ham-D ratio indicates better antidepressant responsiveness (Eq. S3). Ham-D: Hamilton Depression Rating Scale; lPMFG: left posterior middle frontal gyrus; rSup: right supramarginal gyrus; lV1: left primary visual cortex; lMTG: left middle temporal gyrus.

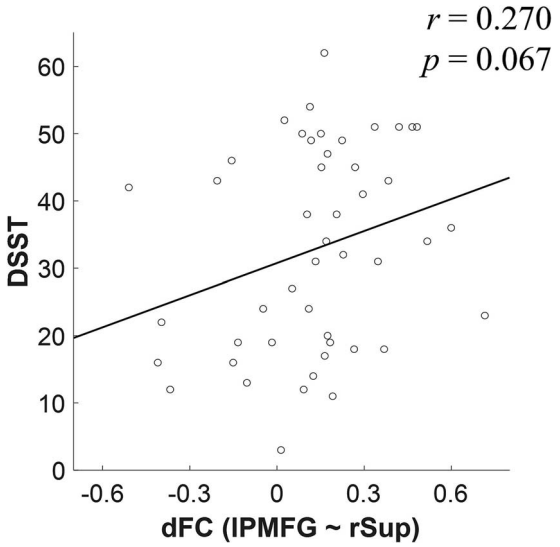

Figure 4. Correlation between the dFC in the lPMFG–rSup and the pre-treatment DSST score. DSST: Digit-Symbol Substitution Test; lPMFG: left posterior middle frontal gyrus; rSup: right supramarginal gyrus.

significant relationship between them. This suggests that the intact cognitive processing speed in patients with MDD may limit the effectiveness of the antidepressants, which is known as the ceiling effect. Notably, a meta-analysis reported that vortioxetine improves cognitive impairment,[57] supporting our findings.

These three core features were consistently selected throughout the validation set except for two samples that shared several characteristics. First, although these two samples were originally classified as rMDD, they were misclassified as such. Second, in the training set, the feature rank of lV1–lMTG was fourth, leading to the selection of an alternative dFC feature, whereas the other two dFC features were commonly selected. Intrigued by this anomaly, we performed an additional classification analysis for these two validation sets using the three core features. Remarkably, these two initially misclassified samples were correctly classified as rMDD. This outcome not only confirms the robustness of the three proposed core features but also highlights the validity of our classification model.

Using only dFC features, we achieved a promising classification performance. Although predicting antidepressant responsiveness using EEG features remains challenging,[14,58] previous ML-based studies have reported an ~80% classification accuracy using PSD-related features (Table S2),[9,10,15-18] which is similar to the performance of our model. However, it should be noted that most of them enhanced classification performance by employing changes in EEG patterns in response to early antidepressant therapy.[9,15-17] Consequently, this approach requires the intake of medicines, potentially leading to acute side effects,[19,20] as well as additional data acquisition, undermining its practicality. More importantly, their performance may be exaggerated owing to several issues, such as erroneous cross-validation-related information leakage and high-dimensionality-related overfitting.[15-17]

In future studies, ML performance could be enhanced by identifying novel and robust biomarkers or determining the optimal biomarker combination. Among previous ML-based studies, Mumtaz et al.[10] achieved the best performance using multi-paradigm baseline EEG features, including resting-state and visual oddball paradigms. Despite using different criteria for treatment responsiveness, their results highlight the potential benefits of expanding the biomarkers to effectively capture the heterogeneous pathophysiological characteristics of patients with MDD.[21] In addition to neurophysiological markers, incorporating demographic, clinical, or genetic characteristics could also improve prediction performance and provide valuable pathophysiological insights. Moreover, employing more sophisticated ML-based models could enhance performance by optimally covering various biomarkers. It should also be noted that further refinement of the extracted features is required, as our HC template-based correlation approach may be suboptimal in fully avoiding data leakage.

Despite its many advantages, this study had some limitations. First, the sample size was not sufficiently large enough to generalize our findings. Due to the limited sample size, we could not validate the proposed performance of the ML using an independent dataset. The small sample size of HC may limit the robustness and generalizability of the constructed normative template. To enhance robustness of our results, further replication studies with diverse cohorts are required. Second, we focused only on the 8-week treatment responsiveness. In future

studies, consideration of other prognostic factors (eg, relapse) could broaden our understanding of its pathophysiology. Third, a placebo control group was not included in the present study. Fourth, there may have been confounding effects of comorbidities in our study. Furthermore, due to data imbalance, we adopted a classification approach for "remission" for each patient, rather than "responsiveness." Fifth, inter-regional gamma-band FC should be carefully interpreted as gamma-band activities are not necessarily linked to direct functional communications[29] as well as vulnerable to noises and artifacts. At the current level of analysis, it remains challenging to delineate the precise neural basis. Finally, as all patients in this study were treated with either vortioxetine or escitalopram, the proposed dFC features might exhibit different performance for predicting effects of antidepressants with different mechanisms.

In this study, we propose that pre-treatment dynamic gamma-band FC responses to salient stimuli could serve as biomarkers for antidepressant responsiveness prediction in patients with MDD. Patients were successfully classified into nrMDD and rMDD groups using three pathophysiological dFC features: lPMFG–rSup, rAng–rAMFG, and lV1–lMTG. Notably, patients with nrMDD exhibit aberrant transient hyperconnections, which may be associated with NMDAR malfunctioning. We hope that the methodology and findings of this study expand the neurobiological understanding of MDD and contribute to neurodynamic biomarker identification.

Acknowledgments

This research was supported by the National Research Foundation (NRF) funded by the Korean government (MSIT) (No. RS-2024-00455484), and by the KBRI basic research program through Korea Brain Research Institute funded by the Ministry of Science and ICT (25-BR-02-02).

Author Contributions

Kang-Min Choi (Conceptualization [lead], Formal analysis [lead], Methodology [lead], Visualization [lead], Writing—original draft [lead]), Taegyeong Lee (Formal analysis [supporting], Methodology [supporting], Writing—review & editing [supporting]), Seung-Hwan Lee (Supervision [equal], Writing—review & editing [equal]), Chang-Hwan Im (Supervision [equal], Writing—review & editing [equal]).

Supplementary Material

Supplementary material is available at *International Journal of Neuropsychopharmacology* (IJNPPY) online.

Funding

None declared.

Conflicts of Interest

The authors have no conflicts of interest to declare.

Data Availability

Due to ethical and privacy considerations, the data are not publicly available. However, they may be provided by the corresponding author upon reasonable request.

References

1. Rolle CE, Fonzo GA, Wu W, et al. Cortical connectivity moderators of antidepressant vs placebo treatment response in major depressive disorder: secondary analysis of a randomized clinical trial. *JAMA Psychiatry* 2020;**77**:397-408. https://doi.org/10.1001/jamapsychiatry.2019.3867
2. Wu H, Liu R, Zhou J, et al. Prediction of remission among patients with a major depressive disorder based on the resting-state functional connectivity of emotion regulation networks. *Transl Psychiatry* 2022;**12**:391. https://doi.org/10.1038/s41398-022-02152-0
3. Braund TA, Tillman G, Palmer DM, Gordon E, Rush AJ, Harris AWF. Antidepressant side effects and their impact on treatment outcome in people with major depressive disorder: an iSPOT-D report. *Transl Psychiatry* 2021;**11**:417. https://doi.org/10.1038/s41398-021-01533-1
4. Heerlein K, Young AH, Otte C, et al. Real-world evidence from a European cohort study of patients with treatment resistant depression: baseline patient characteristics. *J Affect Disord* 2021;**283**:115-122. https://doi.org/10.1016/j.jad.2020.11.124
5. Jaffe DH, Rive B, Denee TR. The humanistic and economic burden of treatment-resistant depression in Europe: a cross-sectional study. *BMC Psychiatry* 2019;**19**:247. https://doi.org/10.1186/s12888-019-2222-4
6. Choi KM, Hwang HH, Yang C, Jung B, Im CH, Lee SH. Association between the functional brain network and antidepressant responsiveness in patients with major depressive disorders: a resting-state EEG study. *Psychol Med* 2025;**55**:e25.
7. Hipp JF, Hawellek DJ, Corbetta M, Siegel M, Engel AK. Large-scale cortical correlation structure of spontaneous oscillatory activity. *Nat Neurosci* 2012;**15**:884-890. https://doi.org/10.1038/nn.3101
8. Rolle T, Ponzetto A, Malinverni L. The role of neuroinflammation in glaucoma: an update on molecular mechanisms and new therapeutic options. *Front Neurol* 2020;**11**:612422. https://doi.org/10.3389/fneur.2020.612422
9. Cook IA, Hunter AM, Caudill MM, Abrams MJ, Leuchter AF. Prospective testing of a neurophysiologic biomarker for treatment decisions in major depressive disorder: the PRISE-MD trial. *J Psychiatr Res* 2020;**124**:159-165. https://doi.org/10.1016/j.jpsychires.2020.02.028
10. Mumtaz W, Xia L, Mohd Yasin MA, Azhar Ali SS, Malik AS. A wavelet-based technique to predict treatment outcome for major depressive disorder. *PLoS One* 2017;**12**:e0171409. https://doi.org/10.1371/journal.pone.0171409
11. Sun J, Ma Y, Guo C, et al. Distinct patterns of functional brain network integration between treatment-resistant depression and non-treatment-resistant depression: a resting-state functional magnetic resonance imaging study. *Prog Neuropsychopharmacol Biol Psychiatry* 2023;**120**:110621. https://doi.org/10.1016/j.pnpbp.2022.110621
12. Zhang Y, Wu W, Toll RT, et al. Identification of psychiatric disorder subtypes from functional connectivity patterns in resting-state electroencephalography. *Nat Biomed Eng* 2021;**5**:309-323. https://doi.org/10.1038/s41551-020-00614-8
13. Kim H, Baik SY, Kim YW, Lee SH. Improved cognitive function in patients with major depressive disorder after treatment with vortioxetine: a EEG study. *Neuropsychopharmacol Rep* 2022;**42**:21-31. https://doi.org/10.1002/npr2.12220
14. Widge AS, Bilge MT, Montana R, et al. Electroencephalographic biomarkers for treatment response prediction in major depressive illness: a meta-analysis. *Am J Psychiatry* 2019;**176**:44-56. https://doi.org/10.1176/appi.ajp.2018.17121358

15. de la Salle S, Jaworska N, Blier P, Smith D, Knott V. Using prefrontal and midline right frontal EEG-derived theta cordance and depressive symptoms to predict the differential response or remission to antidepressant treatment in major depressive disorder. *Psychiatry Res Neuroimaging* 2020;**302**:111109. https://doi.org/10.1016/j.pscychresns.2020.111109
16. Jaworska N, de la Salle S, Ibrahim MH, Blier P, Knott V. Leveraging machine learning approaches for predicting antidepressant treatment response using electroencephalography (EEG) and clinical data. *Front Psychiatry* 2018;**9**:768. https://doi.org/10.3389/fpsyt.2018.00768
17. Zhdanov A, Atluri S, Wong W, et al. Use of machine learning for predicting escitalopram treatment outcome from electroencephalography recordings in adult patients with depression. *JAMA Netw Open* 2020;**3**:e1918377. https://doi.org/10.1001/jamanetworkopen.2019.18377
18. Watts D, Pulice RF, Reilly J, Brunoni AR, Kapczinski F, Passos IC. Predicting treatment response using EEG in major depressive disorder: a machine-learning meta-analysis. *Transl Psychiatry* 2022;**12**:332. https://doi.org/10.1038/s41398-022-02064-z
19. Harmer CJ, O'Sullivan U, Favaron E, et al. Effect of acute antidepressant administration on negative affective bias in depressed patients. *Am J Psychiatry* 2009;**166**:1178-1184. https://doi.org/10.1176/appi.ajp.2009.09020149
20. Machado-Vieira R, Baumann J, Wheeler-Castillo C, et al. The timing of antidepressant effects: a comparison of diverse pharmacological and somatic treatments. *Pharmaceuticals (Basel)* 2010;**3**:19-41. https://doi.org/10.3390/ph3010019
21. Jang KI, Kim S, Chae JH, Lee C. Machine learning-based classification using electroencephalographic multi-paradigms between drug-naive patients with depression and healthy controls. *J Affect Disord* 2023;**338**:270-277. https://doi.org/10.1016/j.jad.2023.06.002
22. Murphy N, Lijffijt M, Ramakrishnan N, et al. Does mismatch negativity have utility for NMDA receptor drug development in depression? *Braz J Psychiatry* 2022;**44**:61-73. https://doi.org/10.1590/1516-4446-2020-1685
23. Askew CE, Metherate R. Synaptic interactions and inhibitory regulation in auditory cortex. *Biol Psychology* 2016;**116**:4-9. https://doi.org/10.1016/j.biopsycho.2015.11.001
24. Atallah BV, Scanziani M. Instantaneous modulation of gamma oscillation frequency by balancing excitation with inhibition. *Neuron* 2009;**62**:566-577. https://doi.org/10.1016/j.neuron.2009.04.027
25. Womelsdorf T, Schoffelen JM, Oostenveld R, et al. Modulation of neuronal interactions through neuronal synchronization. *Science* 2007;**316**:1609-1612. https://doi.org/10.1126/science.1139597
26. Krystal JH, D'Souza DC, Mathalon D, Perry E, Belger A, Hoffman R. NMDA receptor antagonist effects, cortical glutamatergic function, and schizophrenia: toward a paradigm shift in medication development. *Psychopharmacology (Berl)* 2003;**169**:215-233. https://doi.org/10.1007/s00213-003-1582-z
27. Sivarao DV. The 40-Hz auditory steady-state response: a selective biomarker for cortical NMDA function. *Ann NY Acad Sci* 2015;**1344**:27-36. https://doi.org/10.1111/nyas.12739
28. Bastos AM, Vezoli J, Fries P. Communication through coherence with inter-areal delays. *Curr Opin Neurobiol* 2015;**31**:173-180. https://doi.org/10.1016/j.conb.2014.11.001
29. Buzsaki G, Schomburg EW. What does gamma coherence tell us about inter-regional neural communication? *Nat Neurosci* 2015;**18**:484-489. https://doi.org/10.1038/nn.3952
30. Xu Z, Huang J, Liu C, et al. Dynamic functional connectivity correlates of mental workload. *Cogn Neurodyn* 2024;**18**:2471-2486. https://doi.org/10.1007/s11571-024-10101-4
31. Fries P. Neuronal gamma-band synchronization as a fundamental process in cortical computation. *Annu Rev Neurosci* 2009;**32**:209-224.
32. Choi KM, Lee T, Im CH, Lee SH. Prediction of pharmacological treatment efficacy using electroencephalography-based salience network in patients with major depressive disorder. *Front Psychiatry* 2024;**15**:1469645. https://doi.org/10.3389/fpsyt.2024.1469645
33. Williams JB. A structured interview guide for the Hamilton Depression Rating Scale. *Arch Gen Psychiatry* 1988;**45**:742-747. https://doi.org/10.1001/archpsyc.1988.01800320058007
34. Shear MK, Vander Bilt J, Rucci P, et al. Reliability and validity of a structured interview guide for the Hamilton Anxiety Rating Scale (SIGH-A). *Depress Anxiety* 2001;**13**:166-178.
35. Jaeger J. Digit symbol substitution test: the case for sensitivity over specificity in neuropsychological testing. *J Clin Psychopharmacol* 2018;**38**:513-519. https://doi.org/10.1097/JCP.0000000000000941
36. Delorme A, Makeig S. EEGLAB: an open source toolbox for analysis of single-trial EEG dynamics including independent component analysis. *J Neurosci Methods* 2004;**134**:9-21. https://doi.org/10.1016/j.jneumeth.2003.10.009
37. Tadel F, Baillet S, Mosher JC, Pantazis D, Leahy RM. Brainstorm: a user-friendly application for MEG/EEG analysis. *Comput Intell Neurosci* 2011;**2011**:879716. https://doi.org/10.1155/2011/879716
38. Gramfort A, Papadopoulo T, Olivi E, Clerc M. OpenMEEG: open source software for quasistatic bioelectromagnetics. *Biomed Eng Online* 2010;**9**:45. https://doi.org/10.1186/1475-925X-9-45
39. Chen AC, Oathes DJ, Chang C, et al. Causal interactions between fronto-parietal central executive and default-mode networks in humans. *Proc Natl Acad Sci USA* 2013;**110**:19944-19949. https://doi.org/10.1073/pnas.1311772110
40. Toll RT, Wu W, Naparstek S, et al. An electroencephalography connectomic profile of posttraumatic stress disorder. *Am J Psychiatry* 2020;**177**:233-243. https://doi.org/10.1176/appi.ajp.2019.18080911
41. Vinck M, Oostenveld R, van Wingerden M, Battaglia F, Pennartz CM. An improved index of phase-synchronization for electrophysiological data in the presence of volume-conduction, noise and sample-size bias. *Neuroimage* 2011;**55**:1548-1565. https://doi.org/10.1016/j.neuroimage.2011.01.055
42. Yu M. Benchmarking metrics for inferring functional connectivity from multi-channel EEG and MEG: a simulation study. *Chaos* 2020;**30**:123124. https://doi.org/10.1063/5.0018826
43. Quanquan G, Li Z, Han J. Generalized fisher score for feature selection. arXiv:1202.3725, preprint 2012.
44. Curran PJ, West SG, Finch JF. The robustness of test statistics to nonnormality and specification error in confirmatory factor analysis. *Psychol Methods* 1996;**1**:16-29. https://doi.org/10.1037//1082-989x.1.1.16
45. Lee MS, Lee SH, Moon EO. Neuropsychological correlates of the P300 in patients with Alzheimer's disease. *Prog Neuropsychopharmacol Biol Psychiatry* 2013;**40**:62-69. https://doi.org/10.1016/j.pnpbp.2012.08.009
46. Maris E, Oostenveld R. Nonparametric statistical testing of EEG- and MEG-data. *J Neurosci Methods* 2007;**164**:177-190. https://doi.org/10.1016/j.jneumeth.2007.03.024
47. Dudoit S, van der Laan MJ, Pollard KS. Multiple testing. Part I. Single-step procedures for control of general type I error

rates. *Stat Appl Genet Mol Biol* 2004;**3**:Article13. https://doi.org/10.2202/1544-6115.1040

48. Ahmadi H, Fatemizadeh E, Motie-Nasrabadi A. A comparative study of correlation methods in functional connectivity analysis using fMRI data of Alzheimer's patients. *J Biomed Phys Eng* 2023;**13**:125-134. https://doi.org/doi:10.31661/jbpe.v0i0.2007-1134
49. Martens MAG, Filippini N, Harmer CJ, Godlewska BR. Resting state functional connectivity patterns as biomarkers of treatment response to escitalopram in patients with major depressive disorder. *Psychopharmacology (Berl)* 2022;**239**:3447-3460. https://doi.org/10.1007/s00213-021-05915-7
50. Kantrowitz JT, Dong Z, Milak MS, et al. Ventromedial prefrontal cortex/anterior cingulate cortex Glx, glutamate, and GABA levels in medication-free major depressive disorder. *Transl Psychiatry* 2021;**11**:419. https://doi.org/10.1038/s41398-021-01541-1
51. Li CT, Yang KC, Lin WC. Glutamatergic dysfunction and glutamatergic compounds for major psychiatric disorders: evidence from clinical neuroimaging studies. *Front Psychiatry* 2018;**9**:767. https://doi.org/10.3389/fpsyt.2018.00767
52. Kishimoto T, Chawla JM, Hagi K, et al. Single-dose infusion ketamine and non-ketamine N-methyl-d-aspartate receptor antagonists for unipolar and bipolar depression: a meta-analysis of efficacy, safety and time trajectories. *Psychol Med* 2016;**46**:1459-1472. https://doi.org/10.1017/S0033291716000064
53. Fonzo GA, Goodkind MS, Oathes DJ, et al. PTSD psychotherapy outcome predicted by brain activation during emotional reactivity and regulation. *Am J Psychiatry* 2017;**174**:1163-1174. https://doi.org/10.1176/appi.ajp.2017.16091072
54. Leuchter AF, Wilson AC, Vince-Cruz N, Corlier J. Novel method for identification of individualized resonant frequencies for treatment of Major Depressive Disorder (MDD) using repetitive Transcranial Magnetic Stimulation (rTMS): a proof-of-concept study. *Brain Stimul* 2021;**14**:1373-1383. https://doi.org/10.1016/j.brs.2021.08.011
55. Palmiero M, Piccardi L. Frontal EEG asymmetry of mood: a mini-review. *Front Behav Neurosci* 2017;**11**:224. https://doi.org/10.3389/fnbeh.2017.00224
56. Buckner RL, Andrews-Hanna JR, Schacter DL. The brain's default network: anatomy, function, and relevance to disease. *Ann NY Acad Sci* 2008;**1124**:1-38. https://doi.org/10.1196/annals.1440.011
57. Huang IC, Chang TS, Chen C, Sung JY. Effect of vortioxetine on cognitive impairment in patients with major depressive disorder: a systematic review and meta-analysis of randomized controlled trials. *Int J Neuropsychop* 2022;**25**:969-978. https://doi.org/10.1093/ijnp/pyac054
58. Greco C, Matarazzo O, Cordasco G, Vinciarelli A, Callejas Z, Esposito A. Discriminative power of EEG-based biomarkers in major depressive disorder: a systematic review. *IEEE Access* 2021;**9**:112850-112870.

International Journal of Neuropsychopharmacology, 2025, 1–10
https://doi.org/10.1093/ijnp/pyaf042
Regular Research Article